Journal of Proteomics 293 (2024) 105064

Contents lists available at ScienceDirect

Journal of Proteomics

journal homepage: www.elsevier.com/locate/jprot

A comparative urinary proteomic and metabolomic analysis between renal aa amyloidosis and membranous nephropathy with clinicopathologic correlations

Deniz Aral Ozbek [a,*], Sila Cankurtaran Koc [b], Nazlı Ezgi Özkan [c], Sevilay Erdogan Kablan [d], Idil Yet [e], Meral Uner [f], Nurhan Ozlu [c], Emirhan Nemutlu [d], Incilay Lay [g], Arzu Saglam Ayhan [f], Tolga Yildirim [b], Mustafa Arici [b], Seref Rahmi Yilmaz [b], Yunus Erdem [b], Bulent Altun [b]

[a] Hacettepe University Faculty of Medicine, Department of Internal Medicine, Ankara, Turkey
[b] Hacettepe University Faculty of Medicine, Department of Nephrology, Ankara, Turkey
[c] Koc University Research Center for Translational Medicine, Istanbul, Turkey
[d] Hacettepe University Faculty of Pharmacy, Department of Analytical Chemistry, Ankara, Turkey
[e] Hacettepe University Graduate School of Health Sciences, Department of Bioinformatics, Ankara, Turkey
[f] Hacettepe University Faculty of Medicine, Department of Pathology, Ankara, Turkey
[g] Hacettepe University Faculty of Medicine, Department of Biochemistry, Ankara, Turkey

ARTICLE INFO

Keywords:
Amyloidosis
Membranous nephropathy
Metabolomics
Nephrotic syndrome
Proteomics

ABSTRACT

Urinary omics has become a powerful tool for elucidating pathophysiology of glomerular diseases. However, no urinary omics analysis has been performed yet on renal AA amyloidosis. Here, we performed a comparative urine proteomic and metabolomic analysis between recently diagnosed renal AA amyloidosis (AA) and membranous nephropathy (MN) patients. Urine samples of 22 (8 AA, 8 MN and 6 healthy control) patients were analyzed with nLC-MS/MS and GC/MS for proteomic and metabolomic studies, respectively. Pathological specimens were scored for glomerulosclerosis and tubulointerstitial fibrosis grades. Functional enrichment analysis between AA and control groups showed enrichment in cell adhesion related sub-domains. Uromodulin (UMOD) was lower, whereas ribonuclease 1 (RNase1) and α-1-microglobulin/bikunin precursor (AMBP) were higher in AA compared to MN group. Correlations were demonstrated between UMOD-proteinuria ($r = -0.48$, $p = 0.03$) and AMBP-eGFR ($r = -0.69$, $p = 0.003$) variables. Metabolomic analysis showed myo-inositol and urate were higher in AA compared to MN group. A positive correlation was detected between RNase1 and urate independent of eGFR values ($r = 0.63$, $p = 0.01$). Enrichment in cell adhesion related domains suggested a possible increased urinary shear stress due to amyloid fibrils. UMOD, AMBP and myo-inositol were related with tubulointerstitial damage, whereas RNase1 and urate were believed to be related with systemic inflammation in AA amyloidosis.

Significance: Urinary omics studies have become a standard tool for biomarker studies. However, no urinary omics analysis has been performed yet on renal AA amyloidosis. Here, we performed a comparative urinary omics analysis between recently diagnosed renal AA amyloidosis (AA), membranous nephropathy (MN) patients and healthy controls. Pathological specimens were scored with glomerulosclerosis (G) and tubulointerstitial fibrosis (IF) grades to consolidate the results of the omics studies and correlation analyzes. Functional enrichment analysis showed enrichment in cell adhesion related sub-domains due to downregulation of cadherins; which could be related with increased urinary shear stress due to amyloid deposition and disruption of tissue micro-architecture. In comparative proteomic analyzes UMOD was lower, whereas RNase1 and AMBP were higher in AA compared to MN group. Whereas in metabolomic analyzes; myo-inositol, urate and maltose were higher in

Abbreviations: A1M, Alpha-1-microglobulin; *AA*, AA Amyloidosis; *AMBP*, Alpha-1-microglobulin/bikunin Precursor Protein; *ASCVD*, Atherosclerotic Cardiovascular Disease; *CDH*, Cadherin; *CKD*, Chronic Kidney Disease; *eGFR*, Estimated Glomerular Filtration Rate; *FSGS*, Focal Segmental Glomerulosclerosis; *G*, Glomerulosclerosis; *GC/MS*, Gas Chromatography/Mass Spectroscopy; *GO*, Gene Ontology; *IF*, Interstitial Fibrosis; *IgAN*, IgA Nephropathy; *LDL*, Low density Lipoprotein; *Log_2FC*, log2 Fold Change; *MCD*, Minimal Change Disease; *MN*, Membranous Nephropathy; *LC/MS*, Liquid Chromatography/Mass Spectroscopy; *PCA*, Principal Component Analysis; *PLA2R*, Phospholipase 2 Receptor; *PTEC*, Proximal Tubular Epithelial Cell; *RCS*, Renal Chronicity Score; *RNase1*, Ribonuclease 1; *TA*, Tubular Atrophy; *UMOD*, Uromodulin.

* Corresponding author.
E-mail address: araldeniz94@gmail.com (D.A. Ozbek).

https://doi.org/10.1016/j.jprot.2023.105064
Received 27 July 2023; Received in revised form 20 November 2023; Accepted 18 December 2023
Available online 26 December 2023
1874-3919/© 2023 The Authors. Published by Elsevier B.V. This is an open access article under the CC BY-NC-ND license (http://creativecommons.org/licenses/by-nc-nd/4.0/).

AA compared to MN group. Correlations were demonstrated between UMOD-proteinuria ($r = -0.48$, $p = 0.03$), AMBP-eGFR ($r = -0.69$, $p = 0.003$) and between RNase1-Urate independent of eGFR values ($r = 0.63$, $p = 0.01$). This study is the first comprehensive urinary omics analysis focusing on renal AA Amyloidosis to the best of our knowledge. Based on physiologic roles and clinicopathologic correlations of the molecules; UMOD, AMBP and myo-inositol were related with tubulointerstitial damage, whereas RNase1 and urate were believed to be increased with systemic inflammation and endothelial damage in AA amyloidosis.

1. Introduction

AA amyloidosis is a multisystemic amyloidosis subtype that develops on the background of various chronic inflammatory etiologies. The precursor amyloidogenic protein is serum amyloid A (SAA), which is an acute phase reactant found in very low concentrations in normal individuals [1]. Proteinuria is the first clinical presentation in 95% of the cases and nephrotic syndrome is seen in approximately half of these patients, although 10% of the cases can be presented with end-stage renal disease [2,3]. Amyloid deposition must be demonstrated by polarized light microscope for a definitive diagnosis of the disease and mass spectroscopy studies are necessary in cases that are difficult to interpret [4]. Glomerular involvement is almost always present and contribute the nephrotic syndrome [5]. But since amyloid deposition can be seen in any domain of the organ systems, predominantly vascular or tubulointerstitial amyloid infiltrations are also reported in renal AA amyloidosis [6]. Tubulointerstitial inflammation due to amyloid deposition can contribute to proteinuria and is also correlated with worse renal outcomes [7].

Membranous nephropathy (MN) is a prototype autoimmune glomerular disease and the most common cause of idiopathic nephrotic syndrome in non-diabetic adults [8]. While no other underlying disease could be detected in 80% of the cases (Primary MN), the disease is associated with an underlying systemic etiology in 20% of the patients [9]. Autoantibodies developed against M-type phospholipase A2 receptor are detected in 70% of primary MN cases [10]. Regardless of the target antigen, the common pathophysiologic pathway is the accumulation of deposits containing immune complexes beneath the basal surface of the podocyte, which results in glomerular filtration barrier damage and proteinuria [10]. Nephrotic syndrome is detected in 60–80% of the patients, while other patients can be presented with subnephrotic proteinuria [8]. Gold standard of diagnosis is kidney biopsy; although biopsy is not strictly indicated for cases with positive anti-PLA2R antibody and nephrotic syndrome [11].

Proteome and metabolome are defined as whole protein and metabolite content in a given time and biological domain [12]. As urine samples can be easily obtained without any invasive intervention and dynamic nature of proteome and metabolome, urinary proteomic and metabolomic analyzes provide valuable information about biological processes in the kidney and urinary omics studies have become a promising tool for searching pathophysiology, diagnosis and prognosis of glomerular diseases [13]. However, no urinary proteomic and/or metabolomic analysis performed yet focusing on renal AA amyloidosis patients in the literature. Both renal AA Amyloidosis and MN most commonly presents with glomerular involvement and proteinuria. However, in AA Amyloidosis tubulointerstitial involvement can be seen simultaneously and/or predominantly, whereas in primary MN tubular damage is not common especially in early stages of the disease. In this aspect, comparing urine proteomics of AA amyloidosis with MN patients in addition to control group could reveal novel implications. Our main aim in this study is to determine specific urine proteins and metabolites in newly diagnosed renal AA amyloidosis patients with a comparative analysis between membranous nephropathy patients and to investigate correlations of bioinformatic results with clinical and pathological data.

2. Methods

2.1. Patients and control subjects

Study population was selected from adult patients referred to Hacettepe University Department of Nephrology due to proteinuria between January 2021–May 2022. Urine samples were taken after renal biopsy was decided by their primary nephrologist. Patients who were diagnosed with AA amyloidosis and membranous nephropathy after histopathological examination were included in the study.

The exclusion criteria are as follows:

- 24-h urine proteinuria level < 500 mg/day.
- GFR < 15 mL/min/1.73 m^2 or history of renal replacement therapy.
- Previous diagnosis of primary glomerular disease.
- History of immunosuppressive therapy for another disease.
- Presence of acute kidney injury at the time of urine sample collection.
- Pregnant patients.

2.2. Pathological analysis

Renal biopsies of the patients were evaluated independently by two nephropathologists. Pathologic specimens were examined by light and immunofluorescence microscopy. AA amyloidosis diagnosis was made with both Congo red staining and anti-AA antibody positivity in light and immunofluorescence microscopy, respectively. Within the scope of the study, 3 basic histopathological parameters were examined. Glomerular sclerosis (G), tubular atrophy (TA) and interstitial fibrosis (IF) scores were calculated with the percentage of glomeruli with global and segmental sclerosis from all selectable glomeruli and percentage of tubular atrophy and interstitial fibrosis from the total cortical parenchyma respectively. Scores were classified into 4 groups as <10% (none/minimal), 10–25% (mild), 26–50% (moderate) and >50% (severe) and points were assigned according to grade of injury as 0 (none/minimal), 1 (mild), 2 (moderate) and 3 (severe) respectively. Total renal chronicity score (RCS) was calculated as the sum of these scores (G + IF+TA) and classified as minimal (0–1), mild (2–4), moderate (5–7) and severe chronic changes (≥8) [14].

2.3. Proteomic analysis

After hospitalization for renal biopsy, 10 cc mid-stream urine samples were taken between 09.00 and 10.00 a.m., centrifuged at 3200*g* for 15 min at 4 °C and stored at −81 °C.

For the proteomic analysis, urine samples were digested with a modified version of the protocol described in Di Meo et.al [15]. Briefly, urine samples were first clarified by centrifugation at 2000 ×*g* for 10 min at 4 °C, and supernatants were collected for further analysis. After pH adjustment to 8.0 with 0.5 M ammonium bicarbonate (ABC), urine samples were concentrated using 3 K centrifugal filters (Amicon Ultra-15 mL Centrifugal Filters-Ultracek-3) at 4000 g. Concentrated samples were washed with 50 mM ABC and transferred to 10 K filters (Amicon Ultra-0.5 mL Centrifugal Filter Devices, 10 kDa, Millipore, MRCPRT010) for the extensive washing with 50 mM ABC. Ultrafiltrates were then collected and the protein concentration of the samples was determined using BCA assay. Equal amounts of the total protein were used for each

sample. 200 μg of protein for each sample were treated with 8 M urea, 50 mM ABC, and 1 mM sodium orthovanadate, followed by reduction with 100 mM DTT for 45 min at 56 °C and alkylation with 20 mM iodoacetamide (IAA) for 30 min at room temperature in dark. Prior to trypsin addition, samples were diluted 8-fold using 50 mM ammonium bicarbonate and incubated with 20 μg trypsin overnight. Next morning, the reaction was stopped by acidification with 10% formic acid, and digested peptides were desalted using solid phase extraction. 500 ng of digested peptides were analyzed with 90 min gradients in C18 nanoflow reversed-phase high-performance nanometric liquid chromatography (Dionex Ultimate 3000, 3500 RSLC nano, Thermo Scientific) combined with orbitrap mass spectrometer (Q Exactive Orbitrap HF, Thermo Scientific).

2.4. Metabolomic analysis

For the metabolomic analysis, urine samples were digested with a modified version of the protocol described in Eylem et.al [16]. 100 μL of urine samples stored at 20 °C were taken, 50 μL of urease solution (10 mg/5 mL of water) was added each and then incubated for 4 h at 37 °C. 850 μL MeOH:H_2O (9:1, *v*/v) mixture was added and centrifuged at 10000 rpm for 5 min. Samples were evaporated to dryness in vacuum centrifugation at −20 °C until metabolomic analysis was carried out. They were methoxylated for 90 min in a thermal shaker set at 30 °C by adding 20 μL of methoxamine hydrochloride solution. After samples were brought to room temperature, they were derivatized by adding 80 μL of *N*-methyl-*N*-trimethylsilyl trifluoroacetamide and trimethyl chlorosilane (MSTFA +1% TMCS) and left for 30 min at 37 °C in a regulated thermal shaker. The derivatized samples were analyzed by GC–MS. Shimadzu GCMS-QP2010 Ultra device with a DB-5MS stationary phase column was used for metabolomic analysis.

2.5. Bioinformatic analysis

Raw spectroscopic data from nLC-MS/MS analysis was searched in Uniprot database (UP000005640) (https://www.uniprot.org/blast) using MaxQuant proteomics software (version 1.16.14) (http://www.maxquant.org) [17]. Default settings of the Thermo Scientific Q-Exactive HF Hybrid Quadrupole-Orbitrap MS instrument and trypsin/P specificity allowing 2 missing ends were determined as scanning parameters. The minimum peptide length was determined as 7 amino acids and chosen as razor and unique. MaxQuant program completed internal mass calibrations and peptide validations of the measured ions with a false discovery rate of 1%. Label free quantification (LFQ) values were calculated and normalized to the $\log_2$ base. Statistical analysis of the differences in proteins between the study groups were performed with 2-way ANOVA and HSD-Tukey tests using R programming language (version 4.0.4) and logarithmic fold changes ($\log_2$FC) were calculated [18]. Log_2FC value thresholds were chosen as ≥ 3 or ≤ -3 with adjusted p value <0.05 (Benjamini-Hochberg method). Proteins were functionally classified according to biological process, molecular activity and cellular compartment domains with PANTHER classification system (version 17.0) (http://pantherdb.org/) in gene ontology (GO) analysis [19]. Functional enrichment and protein-protein network analyzes were performed using STRING (version 11.5) (https://string-db.org/) [20]. Reactome Knowledgebase (version 83) (https://reactome.org/) was used for pathway analysis [21].

The raw data from GC–MS were converted into mzXML format. MS-DIAL (version 4.60) (http://prime.psc.riken.jp/compms/msdial/main.html) was used for deconvolution and retention time alignment. Peak identification was performed using the retention-indexed Fiehn library. The data were normalized using quality control based on the locally weighted scatterplot smoothing (LOWESS technique and the created data matrices were exported into Excel worksheet [22]. Statistical analysis of the differences in metabolite amounts between the study groups was calculated as described above in proteomic studies using R. Log_2FC thresholds were determined as ≥ 1.5 or ≤ -1.5 with adjusted $p < 0.05$. Functional enrichment analysis of metabolomic studies was made with MetaboAnalyst (version 5.0) (https://www.metaboanalyst.ca/MetaboAnalyst/home.xhtml) [23].

2.6. Statistical analysis

ANOVA, Mann Whitney-U and Kruskal-Wallis tests were used according to the number of groups and distribution characteristics in comparative analyzes. Pearson and Spearman correlation analyzes were used depending on the distribution characteristics of the variables for the relationship of protein/metabolite levels among themselves and with other continuous laboratory parameters. Statistical analysis of the differences in protein and metabolite levels between the study groups were performed with 2-way ANOVA and HSD-Tukey tests and p value was adjusted as <0.05 as detailed above. *Statistical Packages for the Social Sciences* (SPSS Inc. version 26.0) software and R was used for statistical analyzes.

3. Results

3.1. Clinical and demographic parameters

Study included 8 renal AA amyloidosis, 8 membranous nephropathy and 6 healthy control patients. Demographic, clinical and laboratory data of the patients are summarized in Table 1. All of the patients in the AA group were searched for the etiology of amyloidosis. 1 patient had ankylosing spondylitis, 2 patients had refractory chronic infections and 2 patients were clinically diagnosed with familial Mediterranean fever. In comparison between the MN and AA groups, median eGFR values tend to be lower in the AA group (67.6 vs 112 mL/min/1.73 m^2 respectively, $p = 0.08$). Median 24-h urine protein levels did not show a statistically significant difference between the two groups (9499 vs 9512 mg/day respectively, $p = 0.9$).

3.2. Pathological analysis

Pathologic grades and score of the patients were shown in **Table S1**. In comparison between the AA and MN groups, percentages of both moderate and severe TA and IF scores were statistically higher in the AA group ($p = 0.02$). In parallel with these results, moderate and severe G score percentages were higher in the AA group ($p = 0.005$). RCS percentages also showed a significance trend ($p = 0.051$).

3.3. Proteomic analysis

A total of 911 proteins were determined and 859 proteins were included in the bioinformatic analysis of urine samples after filtering

Table 1
Clinical and biochemical results of the patients.

	AA	MN
Age	57,5 (21–76)	42.5 (24–67)
Sex (M/F)	6/2	4/4
Hypertension (%)	%62.5	%62.5
T2DM (%)	%37.5	%12.5
ASCVD (%)	%37.5	%12.5
Creatinine (mg/dL)	1.19 (0.58–4.5)	0.67 (0.41–1.51)
Uric acid (mg/dL)	6.23 (5.3–7.22)	6.59 (3.77–9.3)
Serum albumin (g/dL)	2.41 (1.56–3.48)	2.86 (1.93–3.26)
Proteinuria (mg/day)	9512 (1933–30,120)	9499 (2749–23,977)
eGFR (mL/min/1.73m^2)	67.46 (15.81–127)	112 (46.78–136)
LDL (mg/dL)	153.5 (131–217)	196 (154–273)
Triglyceride (mg/dL)	139 (88–350)	178 (87–596)

Results were expressed as median (min-max) and percentages for each group. AA, MN and C represent AA amyloidosis, membranous nephropathy and control groups, respectively.

due to only identification by one site, potential contamination and reverse columns (Table S2). ANOVA and HSD-Tukey tests showed 51 proteins were differentially expressed between control and AA groups (Table 2). PCA and heatmap analyzes showed that both AA and MN groups could be clearly delineated from control group, although similarity was observed between two groups (Fig. 1).

Three proteins were showed to be statistically different between AA and MN groups. Uromodulin (UMOD) was lower in AA compared to MN group (log_2FC -3.37), whereas RNASE1 (pancreatic ribonuclease) and AMBP (α-1-microglobulin/bikunin precursor protein) were higher in AA compared to MN group (log_2FC 3.41 and 3.07, respectively). In AA and MN patients, Pearson correlation analysis showed statistically significant negative correlations between UMOD-proteinuria ($r = -0.48$, $p = 0.03$) and AMBP-eGFR ($r = -0.69$, $p = 0.003$) variables (Supplementary **Fig. S1**).

Table 2
Proteins and corresponding genes whose levels differ significantly between AA and control group.

Protein	Gene	Log_2 FC (AA/C)
Cadherin-1	CDH1	−5.90
Collagen alpha-1 (VI) chain	COL6A1	−6.23
G-protein coupled receptor family C group 5 member C	GPRC5C	−4.68
Arylsulfatase A	ARSA	−6.38
Alpha-galactosidase A	GLA	−4.29
Lysosomal acid phosphatase	ACP2	−5.79
Interleukin-18-binding protein	IL18BP	−5.49
CD44 antigen	CD44	−7.25
Low affinity immunoglobulin γFc region receptor III-A	FCGR3A	−4.95
Butyrophilin subfamily 2 member A1	BTN2A1	−5.02
ICOS ligand	ICOSLG	−6.19
Prominin-1	PROM1	−4.46
Cubilin	CUBN	−7.04
Peptidoglycan recognition protein 1	PGLYRP1	−4.99
Epidermal growth factor	EGF	−10
Pancreatic alpha-amylase	AMY2A	−8.24
Apolipoprotein D	APOD	−5.26
Plasma serine protease inhibitor	SERPINA5	−5.90
Kallikrein-1	KLK1	−7.14
Uromodulin	UMOD	−8.05
Pepsin A-3; Pepsin A-5; Pepsin A-4	PGA3	−6.48
Non-secretory ribonuclease	RNASE2	−7.63
Aminopeptidase N	ANPEP	−4.76
Cadherin-2	CDH2	−6.38
Gamma-glutamyltranspeptidase 1	GGT1	−4.97
Carboxylic ester hydrolase	CEL	−6.13
Deoxyribonuclease-1	DNASE1	−8.24
Granulins (1–7)	GRN	−5.73
Tyrosine-protein kinase receptor UFO	AXL	−6.13
Endostatin	COL18A1	−6.61
Secreted Ly-6/uPAR-related protein 1	SLURP1	−5.65
Cadherin-13	CDH13	−5.42
Beta-defensin 1	DEFB1	−6.76
Heparan sulfate proteoglycan core protein	HSPG2	−5.02
Low-density lipoprotein receptor-related protein 2	LRP2	−6.38
Galectin-3-binding protein	LGALS3BP	−6.27
WAP four-disulfide core domain protein 2	WFDC2	−5.97
Glutaminyl-peptide cyclotransferase	QPCT	−5.75
Vasorin	VASN	−7.78
CMRF35-like molecule 9	CD300LG	−6.86
Neuronal growth regulator 1	NEGR1	−5.14
Vitelline membrane outer layer protein 1 homolog	VMO1	−5.97
Golgi membrane protein 1	GOLM1	−4.91
Cell adhesion molecule 4	CADM4	−6.27
Roundabout homolog 4	ROBO4	−6.80
Brevican core protein	BCAN	−5.71
Hemicentin-1	HMCN1	−6.46
Endosialin	CD248	−7.17
G-protein coupled receptor family C group 5 member B	GPRC5B	−5.01
Endothelial protein C receptor	PROCR	−7.51
Secreted Ly-6/uPAR-related protein 2	SLURP2	−6.05

The level of all proteins that reached statistical significance were found to be lower in the AA Amyloidosis group than in the control group; therefore, log_2fold values are indicated in the table with a negative sign. AA and C represent AA amyloidosis, membranous nephropathy and control groups, respectively.

3.4. Gene ontology and functional enrichment analyzes

Functional classification results of gene ontology analysis of 51 proteins that significantly differed between AA and control groups was shown in Fig. 2. The sub-domain with the highest gene numbers in biological process domain was cellular process, of which %45.5 was in cellular metabolic process domain. The sub-domain with the highest gene numbers in molecular function domain was binding, of which %85 was in protein binding domain, and the sub-domain with the highest gene numbers in cellular compartment domain was cellular anatomical entity, of which %68.8 was in membrane domain. Classification results showed numerical abundance of adhesion proteins of the cell membrane and catalytic enzymes as these proteins functionally classified in protein binding, membrane and cellular metabolic process domains, respectively.

Functional enrichment analysis of significantly different proteins between AA and control groups were shown in Fig. 3. In cellular compartment domain, proteins that were mainly enriched in catenin complex, lysosomal and vacuolar lumen domains. Cadherin proteins (cadherin-1, cadherin-2 and cadherin-13) were classified in catenin complex. Lysosomal and vacuolar lumen domains included cubilin, granulin, brevican core protein, heparan sulphate proteoglycan core protein-2, acid phosphatase, arylsulfatase A, alpha galactosidase and ribonuclease-2. Due to under expression of urinary cadherin proteins in AA group, cell-cell adhesion related sub-domains were also negatively enriched in biological process domain. Other major proteins classified in cell-cell adhesion related sub-domains were roundabout homolog-4, hemisentin-1, uromodulin, brevican core protein, neuronal growth regulator 1, CD44 and cell adhesion molecule-4. Extracellular matrix constituent and calcium ion binding sub-domains were negatively enriched in molecular function domain. In parallel with functional enrichment analysis results, statistically enriched Reactome pathways were extracellular degradation, integrin cell surface interactions and neutrophil degranulation.

Network analysis of significantly different proteins between AA and control groups were shown in Supplementary **Fig. S2**. Strong protein-protein interactions are evident in network analysis between cadherins, heparan sulphate proteoglycan core protein-2, CD44 and collagen fragment proteins. These proteins were included in cell-cell adhesion related subdomains in biological process and catenin/lysosomal complex subdomains in cellular component domain, respectively. Both domains were negatively enriched in AA group compared to control group in functional enrichment analysis as stated above. Interaction between cadherin proteins, epidermal growth factor, cubulin and megalin were also evident.

3.5. Metabolomic analysis

As a result of metabolomic analysis, a total of 9 metabolites were significantly differed between AA and other groups (Table 3). Spearman correlation analyzes showed significant negative correlation between myo-inositol and eGFR ($r = -0.81$, $p = 0.0002$). Urinary uric acid were not corelated with serum uric acid levels and a negative correlation was also found with eGFR ($r = -0.79$, $p = 0.0003$). In addition, urinary uric acid and myo-inositol levels have a significant positive correlation ($r = 0.95$, $p = 3.35 \times 10^{-16}$). We also searched for possible correlations between proteomic and metabolomic results that could be relevant pathophysiologically in AA Amyloidosis. Significant positive correlation independent of eGFR values was detected between RNASE1 and uric acid ($r = 0.63$, $p = 0.01$).

Enrichment analysis of significant metabolites between the AA,

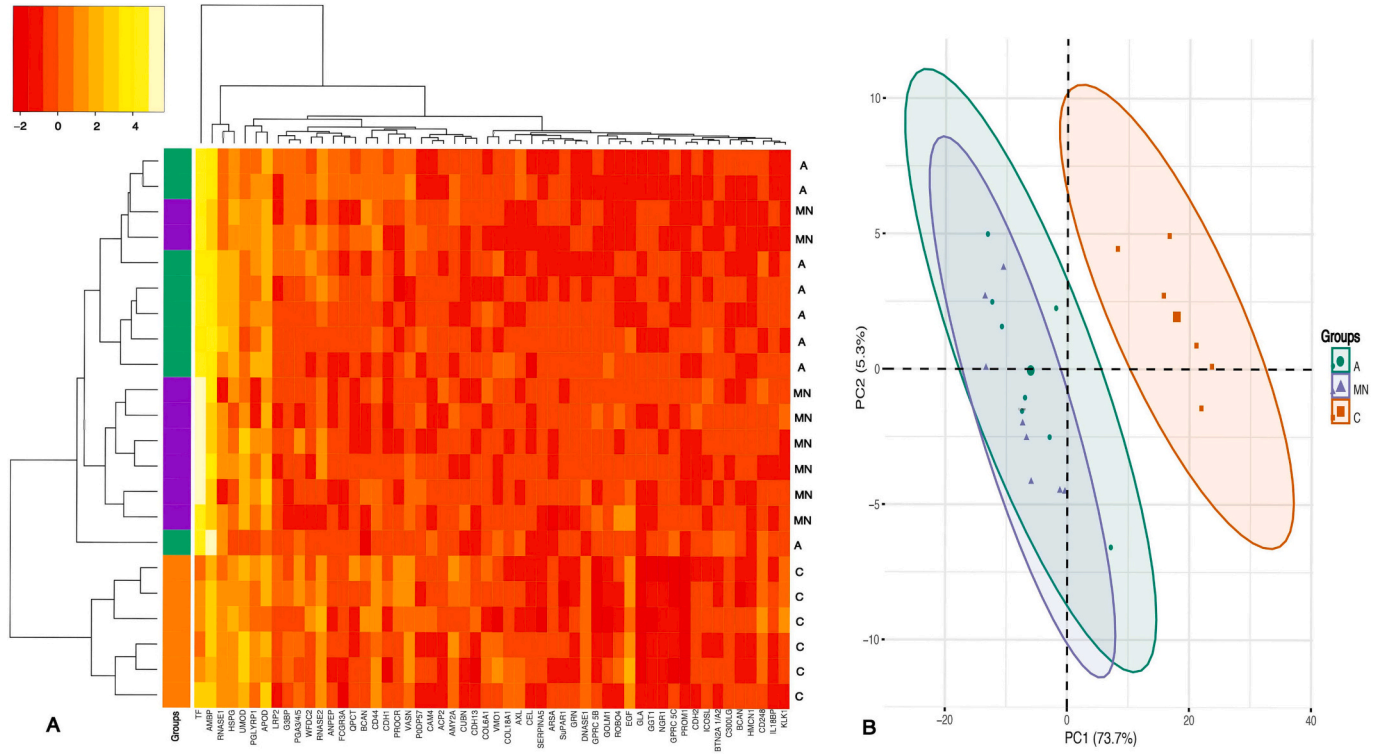


Fig. 1. Heatmap analysis (A) and principal component analysis (B) and of proteomic studies. The color of the cells in heatmap analysis represent the log_2FC value the proteins compared to control group (AA/C and MN/C) and the color encoding with log_2FC intervals is shown on the upper left side of the heatmap.

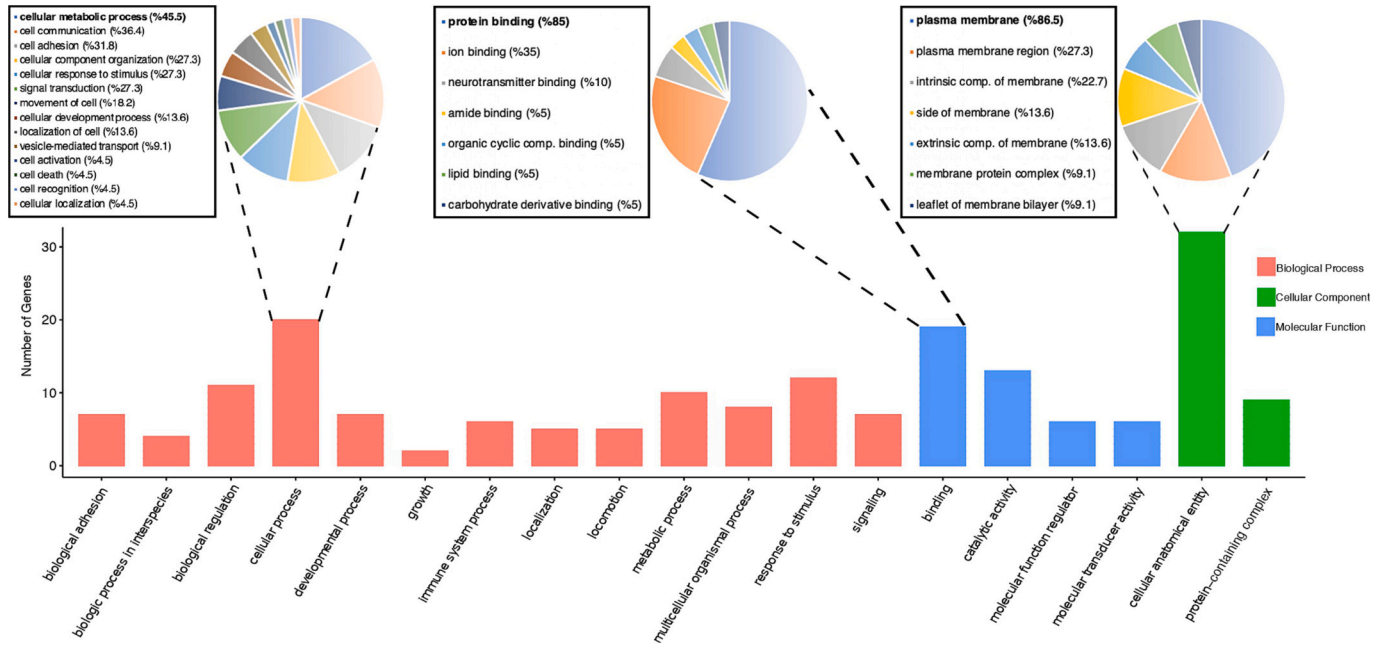


Fig. 2. Gene ontology analysis of proteins that significantly differed between AA and control groups in bar graph and ontologic distributions in major selected domains in pie graphs with PANTHER. Genes that were not assigned with a PANTHER category were filtered. Pie graph distributions were made according to the number of genes in sub-domains, whereas percentages show the percent of gene hits against total gene number in subdomains.

control and the MN groups were made with MetaboAnalyst (Fig. 4). Due to the limited number of organic compounds, pathways were used primarily for functional classification of the metabolites rather than statistical interpretation. Carnitine synthesis pathway had the lowest *p* value (0.0006), while biotin metabolism pathway had the highest enrichment ratio values (21.32) due to L-lysine and trimethyllysine. PCA and heatmap analysis were given in Supplementary **Fig. S3**.

4. Discussion

In this study, a comparative urine proteomic and metabolomic analysis between newly diagnosed renal AA amyloidosis, membranous

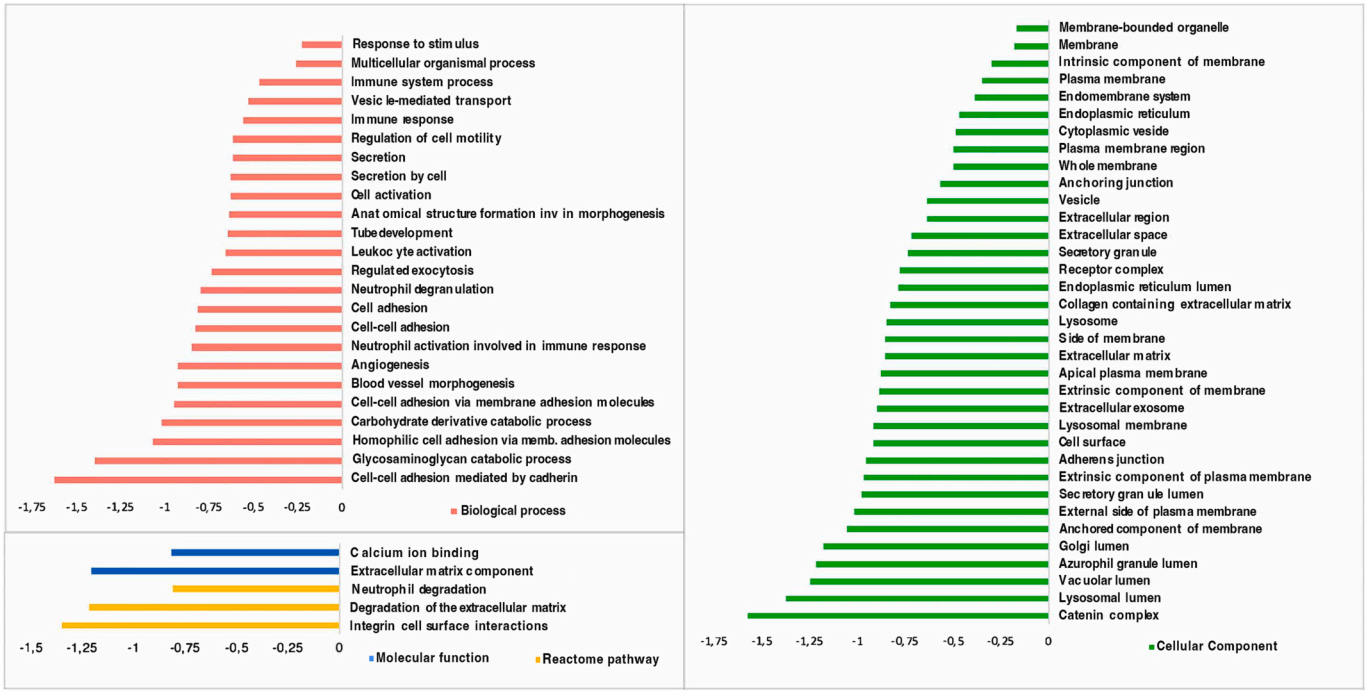


Fig. 3. Functional enrichment analyses of proteins that significantly differed between AA and control groups were performed using STRING online software with a medium confidence level (0.4), providing the significantly enriched GO terms and Reactome pathways. The vertical axis displays the significantly enriched biological functions. The horizontal axis indicates the strength of enrichment, which is the log10 (observed/expected proteins in the network that are annotated with a term). The higher the absolute value of the strength, the stronger the impact.

Table 3
Metabolites with significant differences between AA Amyloidosis and other groups expressed in pairs.

AA/C	AA/MN	MN/C
D-mannitol (3.06)	Myo-inositol (2.18)	Methyl-malonate (−3.1)
Methyl-malonate (−2.96)	Maltose (2.46)	
L-lysine (1.85)	Uric acid (2.65)	
Cysteamine (3.46)		
N-acetylglutamate (2.46)		
Trimethyllysine (−2.65)		

Log_2FC threshold value was determined as ±1.5 and given in parenthesis for each metabolite. AA, MN and C represent AA amyloidosis, membranous nephropathy and control groups, respectively.

nephropathy and healthy control subjects were performed and specific proteins and metabolites that were significantly different in AA amyloidosis group were shown. More specifically, we showed 51 proteins that were significantly lower in AA compared to control group. We also determined discriminating proteins between AA and MN groups: uromodulin was lower, whereas pancreatic ribonuclease and α-1-microglobulin/bikunin precursor protein were higher in AA compared to MN group. We demonstrated and discussed correlations of these molecules with clinicopathological parameters of the patients. Our study is the first urinary comparative omics analysis performed on renal AA amyloidosis patients to the best of our knowledge.

E-cadherin (CDH1), N-cadherin (CDH2) and T-cadherin (CDH13) were lower in AA group compared to the control group, which was reflected in statistically most enriched domains of functional enrichment analysis. In many chronic kidney disease (CKD) etiologies, it was demonstrated that urinary shear stress forces changed due to hyperfiltration, obstruction and hyperviscosity [24,25]. Maggiorani et al. showed that increased urinary shear tension forces changed the characteristics of the tubular epithelium and decreased the expression of CDH1 [26]. In vitro evidence also showed increased vascular shear stress could exacerbate cerebral amyloid fibril deposition process in Alzheimer's disease [27]. Controversial results in terms of relation between urinary and/or serum cadherin levels and CKD were found in the literature, with both increased and decreased urinary CDH1 levels were associated with poor renal outcomes in different cohorts and etiologies [28,29]. Increased amyloid deposition in kidney might theoretically amplificate urinary shear tension forces due to physicochemical properties of amyloid fibrils, although it has not been studied yet specifically in renal amyloidosis. In this context, downregulation of cadherins in AA amyloidosis in comparison to the control group could reflect an increase in urinary shear forces due to amyloid fibrils and these forces may also trigger additional amyloid deposition, thus creating a possible vicious cycle.

Epidermal growth factor (EGF) was lower in AA compared to control group. EGF triggers dimerization by binding to the soluble extracellular domain of the receptor (EGFR), thereby activating intrinsic protein-tyrosine kinase activity [30]. In renal tissue, EGF has various biological functions, including regulation of cellular metabolism and glomerular hemodynamics, modulation of cell growth and post-damage regeneration [31]. Relationship between low urinary EGF levels and high tubulointerstitial fibrosis/low eGFR has been demonstrated in various glomerulonephritis etiologies and urinary EGF has been shown to correlate with healthy renal tubular mass [32–35]. Additionally, as demonstrated in network analysis, there is a close relationship with epidermal growth factor (EGF) and cadherin proteins. Sullivan and colleagues have shown that EGFR and CDH1 dimers were observed as heterotrimers on the epithelial cell membrane at rest which are disrupted by mechanical forces, leading to the release of EGFR and activation of the intracellular signaling pathway in the presence of EGF [36]. In this context, researchers underlined the possible link between shear stress and cell growth. In our study, low urinary EGF level in AA group was thought to be associated with high tubulointerstitial damage due to amyloid accumulation.

Megalin and cubilin were also statistically lower in AA compared to control group. Cubulin and megalin proteins function as membrane-associated endocytic receptors that are responsible for receptor-

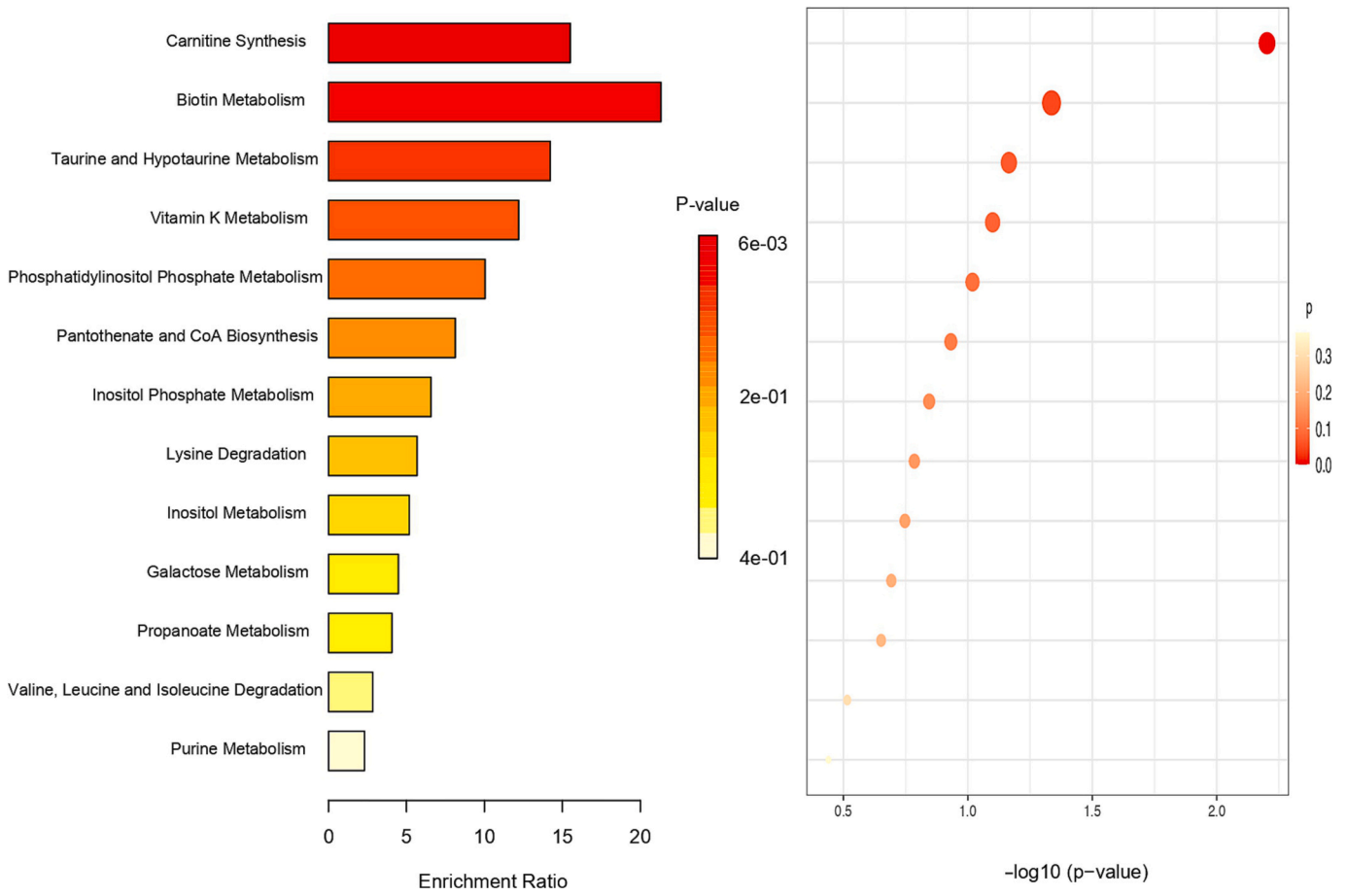


Fig. 4. Functional enrichment analysis significant metabolites between AA, MN and control groups by MetaboAnalyst. In the bar chart (A), the vertical axis displays the significantly enriched biological pathways and the horizontal axis indicates the strength of enrichment, which is the log10 (observed/expected) metabolites in the network that are annotated with a term. Intensity of color indicates lower corrected *p* values. In the dot plot (B), the horizontal axis displays -log10 (*p*-values) of biological pathways, again with higher intensity of the color indicates lower corrected p values.

mediated endocytosis [37]. These highly abundant membrane proteins indirectly reflect health of proximal tubular epithelium cells and tissue expression of megalin was shown to be decreased after toxin and/or ischemia induced renal injuries [38]. There is also evidence for decreased expression of megalin in proximal tubule epithelial cells (PTEC) in proteinuric glomerular diseases [39,40]. Amount of megalin and cubulin proteins in the PTEC membrane do not always correlate with cellular expression. Urinary shedding seems to be the relevant mechanism responsible for reduced levels of these proteins in proteinuric glomerular diseases and regulated intramembrane proteolysis might contribute the link between urinary protein loss and cellular expression levels [39,41]. Studies focused on the urinary megalin/cubilin levels in different CKD etiologies showed increased urinary megalin levels in albuminuric diabetic cohorts whereas decreased levels in Lowe syndrome and Dent's disease [42]. In our study, it is believed that reflected urinary shedding from proximal tubular cells due to proteinuria and low levels of cellular expression due to tubular atrophy, together of which resulted in low urinary megalin and cubulin levels in the AA group that clinically presented with nephrotic syndrome with high amounts of proteinuria.

Pancreatic ribonuclease showed statistically significant difference between the AA and MN groups. RNase1 is an endonuclease belonging to the ribonuclease A superfamily [43]. Although multiple ribonuclease enzymes were known to be found in urine, very scarce data was published on relationship of RNase1 enzyme with kidney diseases [44]. In a comparative urinary proteomic study between patients with FSGS, MN and minimal change disease, RNase1 was reported to be specific for the FSGS group [45]. In a system biology study with a multi-omics approach by Tsalik et al. in 2015, patients with sepsis were categorized according to their renal functions and proteomic, transcriptomic and metabolomic analyzes of plasma samples were performed [46]. Researchers cross-sectionally showed significant correlations between RNase1 with various metabolites related to uremic endothelial damage (phenylacetylglutamine, p-cresol sulfate, D-mannitol) and suggested that increased RNAse1 levels secondary to uremic endothelial damage resulted in RNA destruction, which was supported by positive correlation between RNase1 and uric acid [46]. They postulated that nucleotide degradation products of RNase1 like uric acid further increased endothelial damage. In this context, we suggest that increased expression of RNase1 enzyme in the AA group compared to the MN group might be associated with the underlying systemic and local inflammatory endothelial damage. Increased levels of uric acid and D-mannitol in the AA group compared to the MN and control groups respectively and significant positive correlation between RNase1 and uric acid in amyloidosis patients supported this hypothesis.

Uromodulin was lower and AMBP was higher in AA compared to MN group. UMOD is a glycoprotein that is synthesized only in the cells of the thick ascending arm and early distal tubule compartments of renal tubule; whereas AMBP is a precursor protein that includes bikunin and α-1-microglobulin (A1M) polypeptides, which is easily filtered from the glomerulus and largely reabsorbed from the proximal tubule [47,48]. Both urinary high UMOD and low AMBP/A1M were shown to be indirect biomarkers of healthy nephron volume and a prognostic factor in various CKD etiologies [49–53]. Literature also demonstrated

pathological correlations of urinary UMOD and AMBP levels and tubulointerstitial injury. In a study focusing on the role of urinary markers in determining origin of pathology before kidney biopsy, it was shown that high urinary UMOD level was associated with glomerular etiology in multivariate analysis, indicating a relatively healthy tubular system [54]. It was shown that lower urinary UMOD levels were associated with higher tubular atrophy/interstitial fibrosis scores in IgA nephropathy (IgAN) patients [55]. In a recent study by Melchinger et al. in a large cohort of 364 glomerular diseases, tubular atrophy and interstitial fibrosis were found to be independently associated with urinary UMOD level [56]. In an MS-based comparative analysis performed by Xu et al., it was shown that A1M protein was significantly increased in circulating immune complexes of IgAN patients and A1M protein was also found to be associated with low eGFR levels and tubulointerstitial lesions [57]. In another urinary proteomic analysis of two groups of focal segmental glomerulosclerosis (FSGS) patients with early (eGFR$>$60 mL/min) and advanced (eGFR$<$60 mL/min) stages, AMBP was identified as one of the proteins with the highest $\log_2$FC value in the low GFR group [58].

Amyloid deposition can occur in all compartments of the kidney, whereas in MN immune complex deposition mainly occurs in glomerulus and tubulointerstisium was relatively conserved until late stages of the disease. In this context, relative contribution of glomerular vs tubulointerstitial domains on proteinuric presentations of these disease might be different. In our study tubular atrophy, interstitial fibrosis were statistically higher in AA than in MN group. Therefore, we suggest that low uromodulin and high AMBP levels in AA group is a result of relatively high tubulointerstitial damage in AA amyloidosis at the time of diagnosis.

Although levels of pathophysiologically pivotal proteins which were discussed above were differed between AA and MN groups, significant similar urine proteomics profile was observed in both groups when compared to the control group. This could be explained as although diverse pathways in different nephrotic syndrome etiologies are activated, many of these could be merge upon common and limited ultimate pathways. Multiple proteomics classifiers such as CKD273 have been developed and validated for diagnostic and/or prognostic purposes irrespective of etiology of the renal disease [59–62]. In a large-scale comparative urine proteomic analysis, Siwy et al. shown that in addition to discriminative biomarkers between different glomerular diseases, significant overlap was observed with each CKD etiology and aforementioned proteomic classifiers [63]. Finally, small sample sizes could have also hindered some proteins reaching the threshold.

Metabolomic analyzes showed that levels of myo-inositol and D-mannitol, both of which are members of polyols, were higher in the AA group. Reabsorption of myo-inositol by sodium/myo-inositol transporter proteins (Smit and Smit2) increases in parallel with interstitial osmolarity in healthy medullary cells to protect tubular cells from hyperosmolar damage [64]. In a urinary metabolomic analysis performed by Gill et al. in a large cohort of CKD, it was suggested that Smit protein expression decreased secondary to tubular injury in chronic kidney disease, thus making medullary tubular cells vulnerable to hyperosmolar injury. Authors have been concluded that increased urinary myo-inositol levels were due to the decreased reabsorption [64]. In another ^{1}H NMR-based metabolomics study conducted in CKD patients, urinary myo-inositol levels also found to be increased [65]. In a comparative urinary metabolomics analysis between FSGS and MCD patients, urinary myo-inositol levels were found to be higher in the FSGS group, which was also believed to be associated with higher tubulointerstitial damage and poor prognosis [66]. Urinary myo-inositol/citrate ratio was found to be associated with renal progression in polycystic kidney disease patients [67].

This study has some limitations. Due to the rare incidence of renal AA amyloidosis and inclusion of only newly diagnosed patients, the sample groups were small, which limited generalization of our results. Protein and metabolites detected in omics analyzes could not been confirmed in an independent validation cohort. In addition, cross-sectional nature of the study limits the ability to extrapolate the results for long-term prognosis.

5. Conclusion

Our study is the first urinary omics analysis yet to be performed focusing on renal AA amyloidosis patients. The fact that all the participants were newly diagnosed and therefore had not been received any immunosuppressive treatment decreased possible treatment-related bias. The combination of both proteomic and metabolomic analyzes and histopathologic evaluation of kidney biopsies with validated scoring systems in all patients increased the power of our results. Due to low incidence and underrepresentation of the disease, biomarker studies on CKD patients discussed above could not be generalized in AA amyloidosis unless specific studies designed focusing on the disease. Future studies with larger cohorts and inclusion of validation groups are needed to determine diagnostic and prognostic non-invasive biomarkers in AA amyloidosis.

Supplementary data to this article can be found online at https://doi.org/10.1016/j.jprot.2023.105064.

Funding

This work was supported by grants from Turkish Society of Hypertension and Renal Diseases.

Author contributions

Conceptualization, Deniz Aral Ozbek and Bulent Altun; Data curation, Deniz Aral Ozbek and Sila Cankurtaran Koc; Formal analysis, Deniz Aral Ozbek and Idil Yet; Funding acquisition, Yunus Erdem; Investigation, Deniz Aral Ozbek and Sila Cankurtaran Koc; Methodology, Nazlı Ezgi Özkan, Sevilay Erdogan Kablan, Meral Uner, Nurhan Ozlu, Emirhan Nemutlu, Incilay Lay and Arzu Saglam Ayhan; Project administration, Bulent Altun; Supervision, Tolga Yildirim, Mustafa Arici, Rahmi Yilmaz, Yunus Erdem and Bulent Altun; Writing – original draft, Deniz Aral Ozbek, Tolga Yildirim and Bulent Altun.

Ethics declarations

The study was conducted in accordance with the Declaration of Helsinki and approved by the Institutional Ethics Committee of Hacettepe University (protocol code GO 21/74 and date of approval 21/01/2021). Informed consent was obtained from all subjects involved in the study. This manuscript has been read and approved by all the authors to publish and is not submitted or under consideration for publication elsewhere.

Declaration of Competing Interest

The authors declare that they have no competing interests.

Data availability

The mass spectrometry proteomics data have been deposited to the ProteomeXchange Consortium via the PRIDE partner repository with the dataset identifier *PXD046698*.

Metabolomics data have been deposited to the EMBL-EBI MetaboLights database (DOI: https://doi.org/10.1093/nar/gkz1019, PMID:31691833) with the identifier *MTBLS8909*.

Acknowledgments

Authors would like to thank Mrs. Funda Cakmak for technical support in pre-analytic sample preparations. The authors also gratefully acknowledge the use of the services and facilities of the Koc University

Research Center for Translational Medicine (KUTTAM).

References

[1] I. Sorić Hosman, I. Kos, L. Lamot, Serum amyloid a in inflammatory rheumatic diseases: a compendious review of a renowned biomarker, Front. Immunol. 11 (2021), 631299.
[2] R. Papa, H.J. Lachmann, Secondary, AA, amyloidosis, Rheum. Dis. Clin. 44 (4) (2018) 585–603.
[3] G. Palladini, et al., Prognostication of survival and progression to dialysis in AA amyloidosis, Amyloid: Int. J. Exp. Clini. Invest. Off. J. Int. Soc. Amyloidosis 24 (sup1) (2017) 136–137.
[4] S. Sethi, et al., Laser microdissection and mass spectrometry–based proteomics aids the diagnosis and typing of renal amyloidosis, Kidney Int. 82 (2) (2012) 226–234.
[5] S. Karam, et al., Renal AA amyloidosis: presentation, diagnosis, and current therapeutic options: a review, Kidney Int. 103 (3) (2023) 473–484.
[6] J. Verine, et al., Clinical and histological characteristics of renal AA amyloidosis: a retrospective study of 68 cases with a special interest to amyloid-associated inflammatory response, Hum. Pathol. 38 (12) (2007) 1798–1809.
[7] A. Celtik, et al., A histopathological scoring and grading system to predict outcome for patients with AA amyloidosis, Int. Urol. Nephrol. 52 (2020) 1297–1304.
[8] P. Ronco, et al., Membranous nephropathy, Nat. Rev. Dis. Primers 7 (1) (2021) 69.
[9] W.G. Couser, Primary membranous nephropathy, Clin. J. Am. Soc. Nephrol. 12 (6) (2017) 983–997.
[10] R.A. Sinico, et al., Immunology of membranous nephropathy: from animal models to humans, Clin. Exp. Immunol. 183 (2) (2016) 157–165.
[11] KDIGO, 2021 Clinical Practice Guideline for the Management of Glomerular Diseases, Kidney Int. 100 (4s) (2021) S1–s276.
[12] M. Cañadas-Garre, et al., Proteomic and metabolomic approaches in the search for biomarkers in chronic kidney disease, J. Proteome 193 (2019) 93–122.
[13] M. Provenzano, et al., OMICS in chronic kidney disease: focus on prognosis and prediction, Int. J. Mol. Sci. 23 (1) (2021) 336.
[14] S. Sethi, et al., A proposal for standardized grading of chronic changes in native kidney biopsy specimens, Kidney Int. 91 (4) (2017) 787–789.
[15] A. Di Meo, et al., An integrated proteomic and peptidomic assessment of the normal human urinome, Clin. Chem. Lab. Med. 55 (2) (2017) 237–247.
[16] C.C. Eylem, et al., Untargeted multi-omic analysis of colorectal cancer-specific exosomes reveals joint pathways of colorectal cancer in both clinical samples and cell culture, Cancer Lett. 469 (2020) 186–194.
[17] S. Tyanova, T. Temu, J. Cox, The MaxQuant computational platform for mass spectrometry-based shotgun proteomics, Nat. Protoc. 11 (12) (2016) 2301–2319.
[18] F.M. Giorgi, C. Ceraolo, D. Mercatelli, The R language: An engine for bioinformatics and data science, Life (Basel) 12 (5) (2022).
[19] H. Mi, et al., PANTHER version 16: a revised family classification, tree-based classification tool, enhancer regions and extensive API, Nucleic Acids Res. 49 (D1) (2021) D394–d403.
[20] N.T. Doncheva, et al., Cytoscape StringApp: network analysis and visualization of proteomics data, J. Proteome Res. 18 (2) (2019) 623–632.
[21] B. Jassal, et al., The reactome pathway knowledgebase, Nucleic Acids Res. 48 (D1) (2020) D498–d503.
[22] H. Tsugawa, et al., MS-DIAL: data-independent MS/MS deconvolution for comprehensive metabolome analysis, Nat. Methods 12 (6) (2015) 523–526.
[23] Z. Pang, et al., MetaboAnalyst 5.0: narrowing the gap between raw spectra and functional insights, Nucleic Acids Res. 49 (W1) (2021) W388–w396.
[24] R. Rohatgi, D. Flores, Intra-tubular hydrodynamic forces influence tubulo-interstitial fibrosis in the kidney, Curr. Opin. Nephrol. Hypertens. 19 (1) (2010) 65.
[25] B.M. Grabias, K. Konstantopoulos, The physical basis of renal fibrosis: effects of altered hydrodynamic forces on kidney homeostasis, Am. J. Physiol. Renal Physiol. 306 (5) (2014) F473–F485.
[26] D. Maggiorani, et al., Shear stress-induced alteration of epithelial organization in human renal tubular cells, PLoS One 10 (7) (2015), e0131416.
[27] C.N. Trumbore, Shear-induced amyloid aggregation in the brain: V. Are Alzheimer's and other amyloid diseases initiated in the lower brain and brainstem by cerebrospinal fluid flow stresses? J. Alzheimers Dis. 79 (3) (2021) 979–1002.
[28] R.F. Andersen, et al., Plasma and urine proteomic profiles in childhood idiopathic nephrotic syndrome, PROTEOMICS–Clin. Appl. 6 (7–8) (2012) 382–393.
[29] M. Koziolek, et al., Urine E-cadherin: a marker for early detection of kidney injury in diabetic patients, J. Clin. Med. 9 (3) (2020).
[30] R. Herbst, R.S. Herbst, Review of epidermal growth factor receptor biology, Int. J. Radiat. Oncol. Biol. Phys. 59 (2004) 21–26.
[31] F. Chiarelli, S. Gaspari, M.L. Marcovecchio, Role of growth factors in diabetic kidney disease, Horm. Metab. Res. 41 (8) (2009) 585–593.
[32] L. Wu, et al., Associations of urinary epidermal growth factor and monocyte chemotactic protein-1 with kidney involvement in patients with diabetic kidney disease, Nephrol. Dial. Transplant. 35 (2) (2020) 291–297.
[33] S. Worawichawong, et al., Urine epidermal growth factor, monocyte chemoattractant protein-1 or their ratio as biomarkers for interstitial fibrosis and tubular atrophy in primary glomerulonephritis, Kidney Blood Press. Res. 41 (6) (2016) 997–1007.
[34] A. Segarra-Medrano, et al., Value of urinary levels of interleukin-6, epidermal growth factor, monocyte chemoattractant protein type 1 and transforming growth factor β1 in predicting the extent of fibrosis lesions in kidney biopsies of patients with IgA nephropathy, Nefrología (English Edition) 37 (5) (2017) 531–538.
[35] J.M. Mejia-Vilet, et al., Association between urinary epidermal growth factor and renal prognosis in lupus nephritis, Arthritis Rheum. 73 (2) (2021) 244–254.
[36] B. Sullivan, et al., Mechanical disruption of E-cadherin complexes with epidermal growth factor receptor actuates growth factor-dependent signaling, Proc. Natl. Acad. Sci. U. S. A. 119 (4) (2022).
[37] S. De, S. Kuwahara, A. Saito, The endocytic receptor megalin and its associated proteins in proximal tubule epithelial cells, Membranes 4 (3) (2014) 333–355.
[38] R. Nielsen, E.I. Christensen, H. Birn, Megalin and cubilin in proximal tubule protein reabsorption: from experimental models to human disease, Kidney Int. 89 (1) (2016) 58–67.
[39] H. Fatah, et al., Reduced proximal tubular expression of protein endocytic receptors in proteinuria is associated with urinary receptor shedding, Nephrol. Dial. Transplant. 33 (6) (2018) 934–943.
[40] L. Vinge, et al., The effect of progressive glomerular disease on megalin-mediated endocytosis in the kidney, Nephrol. Dial. Transplant. 25 (8) (2010) 2458–2467.
[41] M. Lal, M. Caplan, Regulated intramembrane proteolysis: signaling pathways and biological functions, Physiology (Bethesda) 26 (1) (2011) 34–44.
[42] T. Seki, et al., Significance of urinary full-length megalin in patients with IgA nephropathy, PLoS One 9 (12) (2014), e114400.
[43] P. Koczera, et al., The ribonuclease a superfamily in humans: canonical RNases as the buttress of innate immunity, Int. J. Mol. Sci. 17 (8) (2016) 1278.
[44] R. Sugiyama, A. Blank, C.A. Dekker, Multiple ribonucleases of human urine, Biochemistry 20 (8) (1981) 2268–2274.
[45] Y.W. Choi, et al., Potential urine proteomics biomarkers for primary nephrotic syndrome, Clin. Proteomics 14 (1) (2017) 1–9.
[46] E.L. Tsalik, et al., Renal systems biology of patients with systemic inflammatory response syndrome, Kidney Int. 88 (4) (2015) 804–814.
[47] A. Lindqvist, et al., Rat alpha 1-microglobulin: co-expression in liver with the light chain of inter-alpha-trypsin inhibitor, Biochim. Biophys. Acta 1130 (1) (1992) 63–67.
[48] C. Schaeffer, O. Devuyst, L. Rampoldi, Uromodulin: roles in health and disease, Annu. Rev. Physiol. 83 (2021) 477–501.
[49] M. Pruijm, et al., Associations of urinary uromodulin with clinical characteristics and markers of tubular function in the general population, Clin. J. Am. Soc. Nephrol. 11 (1) (2016) 70–80.
[50] P.S. Garimella, et al., Urinary uromodulin, kidney function, and cardiovascular disease in elderly adults, Kidney Int. 88 (5) (2015) 1126–1134.
[51] J. Penders, J.R. Delanghe, Alpha 1-microglobulin: clinical laboratory aspects and applications, Clin. Chim. Acta 346 (2) (2004) 107–118.
[52] C.M. O'Seaghdha, et al., Analysis of a urinary biomarker panel for incident kidney disease and clinical outcomes, J. Am. Soc. Nephrol. 24 (11) (2013) 1880–1888.
[53] X. Jiang, et al., Associations of urinary, glomerular, and tubular markers with the development of diabetic kidney disease in type 2 diabetes patients, J. Clin. Lab. Anal. 32 (1) (2018).
[54] A.C. Tran, et al., Urine testing to differentiate glomerular from tubulointerstitial diseases on kidney biopsy, Pract. Lab Med. 30 (2022), e00271.
[55] J. Zhou, et al., Urinary uromodulin excretion predicts progression of chronic kidney disease resulting from IgA nephropathy, PLoS One 8 (8) (2013), e71023.
[56] H. Melchinger, et al., Urine uromodulin as a biomarker of kidney tubulointerstitial fibrosis, Clin. J. Am. Soc. Nephrol. 17 (9) (2022) 1284–1292.
[57] B. Xu, et al., Mass spectrometry-based screening identifies circulating immunoglobulinA-α1-microglobulin complex as potential biomarker in immunoglobulin A nephropathy, Nephrol. Dial. Transplant. 36 (5) (2021) 782–792.
[58] S. Kalantari, et al., Urinary prognostic biomarkers in patients with focal segmental glomerulosclerosis, Nephrourol. Mon. 6 (2) (2014), e16806.
[59] K. Rossing, et al., Urinary proteomics in diabetes and CKD, J. Am. Soc. Nephrol. 19 (7) (2008) 1283.
[60] D.M. Good, et al., Naturally occurring human urinary peptides for use in diagnosis of chronic kidney disease, Mol. Cell. Proteomics 9 (11) (2010) 2424–2437.
[61] C. Pontillo, et al., Prediction of chronic kidney disease stage 3 by CKD273, a urinary proteomic biomarker, Kidney Int. Rep. 2 (6) (2017) 1066–1075.
[62] L. Catanese, et al., A novel urinary proteomics classifier for non-invasive evaluation of interstitial fibrosis and tubular atrophy in chronic kidney disease, Proteomes 9 (3) (2021) 32.
[63] J. Siwy, et al., Noninvasive diagnosis of chronic kidney diseases using urinary proteome analysis, Nephrol. Dial. Transplant. 32 (12) (2017) 2079–2089.
[64] R.B. Gil, et al., Increased urinary osmolyte excretion indicates chronic kidney disease severity and progression rate, Nephrol. Dial. Transplant. 33 (12) (2018) 2156–2164.
[65] S. Qi, et al., A pilot metabolic profiling study in serum of patients with chronic kidney disease based on 1H-NMR-spectroscopy, Clin. Transl. Sci. 5 (5) (2012) 379–385.
[66] J.N. An, et al., Urinary myo-inositol is associated with the clinical outcome in focal segmental glomerulosclerosis, Sci. Rep. 9 (1) (2019) 1–10.
[67] S.E. Dekker, et al., Change in urinary myoinositol/citrate ratio associates with progressive loss of renal function in ADPKD patients, Am. J. Nephrol. (2022) 1–11.